Published in final edited form as:
J Am Chem Soc. 2010 January 27; 132(3): 1098–1109. doi:10.1021/ja908851e.

EPR and Mössbauer Spectroscopy Show Inequivalent Hemes in Tryptophan Dioxygenase

Rupal Gupta[†], **Rong Fu**[§], **Aimin Liu**[‡], and **Michael P. Hendrich**[†]
Department of Chemistry, Carnegie Mellon University, Pittsburgh, Pennsylvania 15213, and Department of Chemistry, Georgia State University, Atlanta, Georgia 30303

Michael P. Hendrich: hendrich@andrew.cmu.edu

Abstract

Tryptophan 2,3-dioxygenase (TDO) is an essential enzyme in the pathway of NAD biosynthesis and important for all living organisms. TDO catalyzes oxidative cleavage of the indole ring of L-tryptophan (L-Trp), converting it to *N*-formylkynurenine (NFK). The crystal structure of TDO shows a dimer of dimer quaternary structure of the homotetrameric protein. The four catalytic sites of the protein, one per subunit, contain a heme that catalyzes the activation and insertion of dioxygen into L-Trp. Because of the α_4 structure and because only one type of heme center has been identified in previous spectroscopic studies, the four hemes sites have been presumed to be equivalent. The present work demonstrates that the heme sites of TDO are not equivalent. Quantitative interpretation of EPR and Mössbauer spectroscopic data indicates the presence of two dominant inequivalent heme species in reduced and oxidized states of the enzyme, which is consistent with a dimer of dimer protein quaternary structure that now extends to the electronic properties of the hemes. The electronic properties of the hemes in the reduced state of TDO change significantly upon L-Trp addition, which is attributed to a change in the protonation state of the proximal histidine to the hemes. The binding of O_2 surrogates NO or CO shows two inequivalent heme sites. The heme–NO complexes are 5- and 6-coordinate without L-Trp, and both 6-coordinate with L-Trp. NO can be selectively photodissociated from only one of the heme–NO sites and only in the presence of L-Trp. Cryoreduction of TDO produces a novel diamagnetic heme species, tentatively assigned as a reduced heme-OH complex. This work presents a new description of the heme interactions with the protein, and with the proximal His, which must be considered during the general interpretation of physical data as it relates to kinetics, mechanism, and function of TDO.

Introduction

Tryptophan 2,3-dioxygenase (TDO) catalyzes oxidative cleavage of the indole ring of L-tryptophan (L-Trp), converting it to *N*-formylkynurenine (NFK). TDO utilizes a *b*-type

Correspondence to: Michael P. Hendrich, hendrich@andrew.cmu.edu.
[†]Carnegie Mellon University.
[‡]Georgia State University.
[§]Current address: Department of Neurology, Emory University, Atlanta, GA 30322.

Supporting Information Available: Complete ref 13. This material is available free of charge via the Internet at http://pubs.acs.org.

heme to catalyze the first committed step for L-Trp degradation through the kynurenine pathway.[1–7] The kynurenine pathway constitutes the major route of de novo biosynthesis of NAD, one of the essential redox cofactors in all living systems.[1] The alteration of intermediate metabolites of this pathway can lead to numerous physiological and pathological conditions, including cataract formation, cerebral malaria, Alzheimer's disease, HIV infection, Huntington's disease, and ischemic brain injury.[2–5] TDO is responsible for oxidizing over 99% of the free L-Trp in intracellular and extracellular pools.[2] In addition, the levels of tryptophan regulated by TDO can affect the synthesis of serotonin,[2,8–10] a known neurotransmitter.

Hemoproteins perform a wide range of biological functions including oxygen transport, storage, electron transfer, monooxy-genation, and reduction of dioxygen; however, they rarely express a dioxygenase activity as their native biological function. TDO is the first described exception.[7,11,12] As an oxygenation enzyme, TDO and its orthologue, indoleamine 2,3-dioxygenase (IDO), are distinctive members of the dioxygenase family in that they utilize a histidine-ligated ferrous heme rather than a nonheme iron or manganese to carry out the oxygen activation and insertion.[13–15]

A number of recent biochemical and spectroscopic studies on substrate recognition have clarified the role of the active site environment.[16–21] The heme binding site of TDO has only one axial position for O_2 binding and activation,[13,14,16] and the primary substrate, L-Trp, must bind to a pocket adjacent to the Fe ion.[13] The crystal structures of TDO from *Xanthomonas campestris* and *Ralstonia metallidurans* show each monomer of the homotetramer with a *b*-type heme.[13,14,22] The substrate binding pocket of one monomer is composed of amino acids from a second monomer to give a dimer of dimer quaternary structure for the homotetramer. In the absence of L-Trp, the oxidized and reduced enzymes contain high-spin hemes. The ferric heme of oxidized TDO is 6-coordinate with axial coordination to the iron from the proximal His and water.[23,24] The ferrous heme of reduced TDO is 5-coordinate,[17] as expected for a high-spin ferrous heme in which the Fe moves out of the porphyrin plane toward the proximal His to give square pyramidal geometry.

A number of studies have shown that L-Trp, or other exogenous molecules, or pH changes affect the electronic properties of the hemes. For example, in the presence of L-Trp, a low-spin site with a hydroxide axially coordinated to the heme is observed.[17,19,23] These changes in electronic properties have been interpreted as due to either equilibria or heterogeneity in the context of four equivalent hemes per homotetramer.

In this work, EPR and Mössbauer spectroscopy of the oxidized and reduced states of TDO from *Ralstonia metallidurans* are presented, with and without substrate, and the O_2 surrogates NO and CO. The data indicate the presence of two dominant inequivalent heme species in multiple states of the enzyme, which is consistent with a dimer of dimer protein quaternary structure that is extended to the electronic properties of the hemes. This intrinsic electronic inequivalence of the hemes in TDO is new, and although the presence of the substrate L-Trp affects the hemes, it is not responsible for the electronic difference in the hemes. The spectroscopy also indicates that the electronic properties of the hemes in the reduced state of TDO change significantly upon L-Trp addition, consistent with a change in

the protonation state of the proximal histidine to the hemes. Data from cryoreduction of oxidized TDO are presented, which allows correlation of states of the enzyme and shows a novel heme species.

Materials and Methods

Preparation of TDO

The construction of the plasmid encoding full-length *Ralstonia metallidurans* TDO has been described elsewhere.[1,14] The ^{56}Fe-containing TDO was prepared by growing the *E. coli* culture with LB medium supplemented with δ-aminolevulinic acid and ammonium ferrous sulfate prior to induction. Filtration and low-speed centrifugation were used in the protein purification to avoid loss of the heme Fe prosthetic group. TDO was obtained by using a 100 mL HiLoad nickel-affinity column and a Superdex 200 gel-filtration column on an ÅKTA FPLC system. The purified enzyme has 60–65% heme Fe occupancy based on the determination of protein concentration and Fe-content using inductively coupled plasma optical emission spectroscopy and EPR spectroscopy. The optical absorption spectrum of the TDO enzyme used in this work displays a $405_{nm}/280_{nm}$ ratio of approximately 1.4:1. The purified enzyme demonstrated a specific activity of 25 μmol/min/mg.

The ^{57}Fe-enriched TDO was obtained by growing cell culture with metal-depleted medium supplemented with ^{57}Fe. The ^{57}Fe stock solution was prepared by dissolving the ^{57}Fe-enriched metal foil (95% ^{57}Fe-enrichment) in concentrated sulfuric acid under O_2-free condition. The pH of the ^{57}Fe stock solution was raised to about 3–5 by an argon-saturated NaOH solution. The culture medium was forced through a Chelex-100 column prior to the addition of ^{57}Fe at the final concentration of 40 μM.

Sample Preparation

All anaerobic protein samples were prepared by degassing protein solutions on a gas manifold using hydrated nitrogen gas from liquid N_2 exhaust. The solutions were exposed to a mild vacuum for 10 s and then purged with N_2 gas. This process was repeated at least six times for each sample. The EPR samples were held horizontally while in the sample tube to expose a greater surface area. Anaerobic transfers were made using gastight Hamilton syringes. The buffer in all samples was 50 mM Tris-HCl (Bio-Rad), pH 7.4, 10% glycerol, unless otherwise noted. Degassed buffers were prepared similarly, except that the vacuum above the solution was brought to 5 μTorr. L-Trp (Sigma) was added to various EPR and Mössbauer samples of TDO in at least 10-fold excess over protein concentration unless otherwise noted. The addition of L-Trp to the reduced samples was made with degassed buffer containing L-Trp. Samples of TDO were reduced by the addition of degassed buffer containing 1–2 equiv of sodium dithionite (EMD) to the degassed protein samples. The exchange of buffers to pH 6.0 or 8.4 was performed with 100 KDa Centricons. Cryoreduction of oxidized TDO was performed by irradiating the protein while in the Mössbauer cup with a ^{60}Co source (dose 50 kGy) for 5 h at 77 K.

Buffer saturated with NO gas was prepared by delivering quantitative amounts of the NO donor diethylamine NONOate (Na hydrate, 15 min half-life, Sigma) to degassed buffer

under anaerobic conditions. The solution was allowed to react for 25 min. Measured volumes of this buffer were added to the anaerobic ferrous protein solution using gastight Hamilton syringes. An excess of CO gas (Aldrich) was delivered to anaerobic ferrous Mössbauer samples with and without L-Trp by gentle bubbling of the gas into the protein solution for 20 min.

Spectroscopy

X-band (9.62 GHz) EPR spectra were recorded on a Bruker 300 spectrometer equipped with an Oxford ESR-910 liquid helium cryostat. Q-band (34.21 GHz) EPR spectra were recorded on a Bruker 200 spectrometer with a home-built microwave probe and cryostat.[25] The quantification of all signals is relative to a CuEDTA spin standard. For both instruments, the microwave frequency was calibrated with a frequency counter and the magnetic field with a NMR gaussmeter. The sample temperature of the X-band cryostat was calibrated with a carbon-glass resistor (LakeShore CGR-1-1000) placed at the position of the sample in an EPR tube. The sample temperature in the Q-band cryostat was determined from calibrated carbon-glass sensors positioned above and below the sample cavity. A modulation frequency and amplitude of 100 kHz and 1 mTpp was used for all EPR spectra, except for the spectra of the NO adduct which used 0.1 mTpp. The EPR simulation software was written by one of the authors.[26] The software diagonalizes the spin Hamiltonian $H = \beta_e \mathbf{B} \cdot \mathbf{g} \cdot \mathbf{S} + \mathbf{S} \cdot \mathbf{D} \cdot \mathbf{S} + \mathbf{S} \cdot \mathbf{A_1} \cdot \mathbf{I_1} + \mathbf{S} \cdot \mathbf{A_2} \cdot \mathbf{I_2}$, where the parameters have the usual definitions, and $\mathbf{I_1}$ and $\mathbf{I_2}$ refer to the nuclear spin of ^{14}N. The simulations are least-squares fits of the experimental spectra generated with consideration of all intensity factors, which allows computation of simulated spectra for a specified sample concentration. The simulations therefore allow a quantitative determination of protein signal intensities. The Windows software package (SpinCount) is available for general application to any mono- or dinuclear metal complex by contacting M. Hendrich.

Mössbauer spectra were recorded with two spectrometers, using Janis Research Super-Varitemp dewars, that allowed studies in applied magnetic fields up to 8.0 T in the temperature range from 4.2 to 200 K. Isomer shifts are reported relative to Fe metal at 298 K. The Mössbauer spectra showing magnetic splittings were calculated using the spin Hamiltonian:

$$H=\beta_e\mathbf{B}\cdot\mathbf{g}\cdot\mathbf{S}+\mathbf{S}\cdot\mathbf{D}\cdot\mathbf{S}+\mathbf{S}\cdot\mathbf{A}\cdot\mathbf{I}-g_n\beta_n\mathbf{B}\cdot\mathbf{I}+(eQV_{zz}/12)[3I_z^2-I(I+1)+\eta(I_x^2-I_y^2)$$

Least-square fitting of the spectra was performed with the WMOSS software package (WEB Research, Edina, MN).

Results

Oxidized TDO

The EPR spectrum of oxidized (as isolated) TDO in 50 mM Tris, pH 7.4, is shown in Figure 1A. The spectrum shows signals near g = 6 and 2, which are typical of high-spin heme centers with approximate axial symmetry. The simulation shown in Figure 1B is calculated for S = 5/2, E/D = 0.0095. The spin concentration of this signal is in quantitative agreement

with the heme concentration determined spectrophotometrically. The titration of this sample with L-Trp (Figure 1C–E) shows that maximal loss (65%) of the concentration of the high-spin signal of Figure 1A was achieved with 50 equiv of L-Trp. The high-spin signal also changes in shape to a more axial heme species with $E/D = 0.006$. The decrease in the intensity of the high-spin heme signal is quantitatively accounted for by the appearance of three new species: majority low-spin (o1-Trp-OH, **g** = (1.80, 2.19, 2.69)), minority low-spin ($g_{max} = 2.61$), and minority high-spin ($g = 6.63$). The g-values of o1-Trp-OH give crystal field parameters (Table 1) indicative of axial coordination of the ferric heme with histidine and hydroxide.[27]

Similar spectra of oxidized TDO have been reported previously;[19] however, an accurate determination of the species amounts has not been reported. Figure 1B and F shows simulations of the spectra with and without L-Trp, respectively. The parameters of each species and the relative amounts are given in Table 1. The signal due to nonheme iron species ($g = 4.3$) is from a contaminant amounting to less than 1% of the iron and is not considered further. The majority low-spin and high-spin species will be referred to as o1-Trp-OH and o2-Trp, respectively. Four different sample preparations from two different protein purification preparations gave percentage amounts of all species that varied by no more than the uncertainties listed in Table 1.

Upon buffer exchange to 50 mM MES, pH 6.0, the EPR spectrum (Figure 2A) changes to a signal that is nearly identical to that of species o2-Trp at pH 7.4. At pH 6.0, as shown in Figure 2B, the addition of L-Trp to this sample did not generate the low-spin Fe(III)–OH species (o1-Trp-OH). However, upon return of the buffer to pH 7.4, the species o1-Trp-OH is again observed (Figure 2C), and approximately in the same ratio of amount with o2-Trp as observed in Figure 1D. Upon buffer exchange to 50 mM Tris, pH 8.4, the EPR spectrum (not shown) is unchanged relative to that at pH 7.4. The addition of L-Trp at pH 8.4 produced the same changes to the EPR spectra as that observed at pH 7.4.

Low-temperature (4.2 K) Mössbauer spectra of ^{57}Fe enriched TDO in magnetic fields of 8 T and 45 mT, parallel to the γ-rays, are shown in Figure 3A,B. At 4.2 K, the oxidized state of the protein shows a single six-line magnetic pattern. The simulations overlaid on the data (solid lines) are calculated for an $S = 5/2$ iron site with $\delta = 0.42(1)$ mm/s, $\Delta E_Q = 1.53(1)$ mm/s, $\eta = 0$, $D = 12.5$ cm^{-1}, $E/D = 0.01$, and $A_{iso} = -195$ kG. These values are indicative of high-spin ferric heme.[27] The high-field Mössbauer spectra are sensitive to small variations in D. A slightly better fit of Figure 3A is obtained with two species in equal amounts for $D =$ 10 and 15 cm^{-1}.

The addition of L-Trp to oxidized TDO results in the conversion of 60% of the high-spin species to a low-spin ferric species (Figure 3C). The spectrum of the low-spin species (Figure 3D) is shown for the difference, (C) – 0.4 (B). The spectrum of Figure 3D is typical of low-spin heme species, which are complicated by the presence of a large anisotropy of the hyperfine tensor.[28] The ratio of low-spin to high-spin species from the Mössbauer spectra is in agreement with the EPR data. Thus, the low-spin heme species of Figure 3C is the hydroxide adduct (species o1-Trp-OH).

Reduced TDO

Anaerobic samples of TDO were reduced with sodium dithionite, and the Mössbauer spectrum of a sample, recorded at 4.2 K in a magnetic field of 45 mT parallel to the γ-rays, is shown in Figure 4A. Three different protein preparations gave the same spectra as shown in Figure 4. The spectrum of Figure 4A consists of a broad outer doublet and a minor inner doublet. The fit shown on the data of Figure 4A contains two major species (r1, r2) and a minor species (r-minor) as noted in Figure 4A, with parameters given in Table 2. The major species constitute in sum 80% of the iron, and the minor species (r-minor) contains 20% of the iron. The line width of the major species is 0.4 mm/s, which is broad but acceptable for single ferrous species. This fit is not unique due to the lack of resolution of species, but it is the minimal number of species, and the relative amounts of the major and minor species are determined. The isomer shifts and quadrupole splittings of all species are in the range typical of high-spin ferrous (S = 2) heme proteins.[28]

The Mössbauer spectrum after the addition of 10 equiv of L-Trp to reduced TDO under anaerobic conditions is shown in Figure 4B, which was also reproduced in three samples. A large and relatively sharp absorption is now observed. At T = 100 K (not shown), the Mössbauer spectrum is essentially unchanged. The difference spectrum (B)–(A) (Figure 4C, for equal areas of (A) and (B)) shows that partial loss of the broad outer absorption feature contributes to the area of the sharp inner doublet in the presence of L-Trp. The fits shown in Figure 4B and C minimally require three doublets: a sharper inner doublet (r2-Trp, δ = 0.95 mm/s, ΔE_Q = 2.54 mm/s) containing 65% of the iron, and two outer doublets (r1-Trp, δ = 1.0 mm/s, ΔE_Q = 3.1 and 3.6 mm/s), which in sum contain 35% of the iron.

There are two plausible interpretations for the change in the spectra upon addition of L-Trp. (1) The quadrupole splitting of one major species changes from 3.8 mm/s (r2) to 2.54 mm/s (r2-Trp). The total iron content in this doublet (65%, ΔE_Q = 2.54 mm/s) is the sum: 45% of the iron from r2 (prior to L-Trp) plus the underlying 20% minority species present without L-Trp (assumed to be unchanged). Species r1 changes with addition of L-Trp to r1-Trp, which is heterogeneous and constitutes 35% of the iron, but the change is not as significant as that of species r2. (2) The electronic properties of both species (r1, r2) change significantly, and both contribute to the doublet with the lower value of ΔE_Q = 2.54 mm/s. This latter interpretation implies that L-Trp only partially converts both species, as significant absorption remains from the original species after L-Trp addition. However, the Mössbauer samples contain much more than enough L-Trp to fully bind the sites with L-Trp (K_d = 4 μM[13]). Consequently, the first interpretation is favored and listed in Table 2. The first interpretation is also supported by cryoreduction of TDO (presented below), which shows two species in equal amounts with ΔE_Q = 2.54 and 3.31 mm/s. Furthermore, the selective loss of NO by photodissociation (presented below) from only one of the major species results in the generation of a reduced heme species with a quadrupole splitting of ΔE_Q = 2.54 mm/s.

The isomer shifts and quadrupole splittings of all species with L-Trp are in the range typical of high-spin ferrous (S = 2) heme proteins.[28] The spectra of the reduced samples, with or without L-Trp, show no evidence of ferric heme species, indicating full reduction of the

samples. The signs of ΔE_Q could not be determined due to the presence of multiple species in high magnetic field spectra.

Cryoreduction of the Oxidized State

A sample of oxidized TDO in a Mössbauer sample cup was placed in a ^{60}Co source (dose 50 kGy) γ-ray source for 5 h at 77 K. Prior to the γ-ray exposure, the Mössbauer spectrum of the sample was the same as that of Figure 3B, indicating all iron was in the ferric state. The Mössbauer spectrum after γ-ray exposure is shown in Figure 5A. The spectrum indicates that 50% of the sample has been reduced and the remainder is unchanged. After subtraction of the starting spectrum, the difference spectrum (Figure 5B) shows two sharp doublets, indicating homogeneous species, each containing 25% of the total iron in the sample. The parameters for these species, o1^{red}-OH and o2^{red}, are determined from the fit shown on the data, labeled OH and 2, and given in Table 2. The parameters of the outer doublet, species o2^{red}, match that of reduced TDO with L-Trp (r2-Trp), although L-Trp is not present in the sample. The inner doublet, species o1^{red}-OH, is from a novel heme complex. Figure 5C shows the Mössbauer spectrum of this sample in a magnetic field of 8 T after subtraction of the starting spectrum. This spectrum is complicated by the presence of the high-spin Fe(II) species from the other site, but it is clear from the diamagnetic simulation overlaid on the data that this sample contains a diamagnetic (S = 0) species in an amount equal to the novel heme species. The parameters of this doublet are not typical of any known heme protein species or porphyrin complex. The two species observed after cryoreduction are referred to as o1^{red}-OH and o2^{red} for reasons to be given in the Discussion.

The cryoreduced sample was annealed at 180 K for 15 min. The spectrum after annealing showed no change in the ferric species, and this has been subtracted from the resulting spectrum shown in Figure 5D. The fit shown on the data indicates two sites, labeled o1^{red}-anneal and o2^{red}-anneal, with parameters given in Table 2. The annealing resulted in nearly complete loss of the S = 0 species o1^{red}-OH, and a corresponding appearance of a species with the same parameters as of one of the major species of reduced TDO (r1, ΔE_Q = 3.31 mm/s), whereas o2^{red} (ΔE_Q = 2.54 mm/s) did not change. The sample was thawed under nitrogen for 3 min and refrozen. The resulting spectrum after subtraction of the ferric species is shown in Figure 5E. After the sample was thawed, the amount of the ferric heme species decreased by 10%, indicating some further reduction of the hemes, presumably from trapped free radicals. The thawing of the sample resulted in the loss of the o2^{red} species and the appearance of an absorption with ΔE_Q = 3.8 mm/s, which is associated with the other major species of reduced TDO (r2, ΔE_Q = 3.8 mm/s). The difference spectrum after thawing is close to the spectrum of reduced TDO, which is overlaid on the spectrum.

CO Addition to Reduced TDO

CO was added under anaerobic conditions by bubbling CO gas into a reduced TDO sample with or without L-Trp. Figure 6A shows the Mössbauer spectrum after CO addition to the L-Trp sample, on a narrow velocity scale to enhance resolution. The spectrum after CO addition without L-Trp is nearly identical. All ferrous species are quantitatively converted to two new doublets due to CO binding to the hemes. The fit shown in Figure 6A requires two quadrupole doublets containing equal amounts of iron with parameters given in Table 2 for

species r_a-CO and r_b-CO. This fit is supported by the Fourier filtered spectrum (Figure 6B) for which the intrinsic ^{57}Fe source line width has been removed to allow resolution of the two doublets. The parameters with or without L-Trp are the same. The parameters of these doublets are typical of diamagnetic CO adducts of ferrous hemes.[28] Fourier filtering of the spectra of reduced TDO without CO, that is, the spectra of Figure 4, did not produce resolved doublets.

NO Addition to Reduced TDO

X- and Q-band EPR spectra of reduced TDO after additions of buffer saturated with NO from NONOates are shown in Figure 7A and E, respectively. The total amount of NO added to the sample was approximately 2 equiv. The spectra clearly contain two distinct $S = 1/2$ rhombic species from heme–NO adducts. Simultaneous least-squares fits of the spectra produced the simulations shown in Figure 7B and F for the two microwave frequencies, both with the same parameter set given in Table 1 for species r1-NO and r2-NO. The best fits to the data require equal concentrations for the two species. The ratio of the two species can change by no more than 5% before the resulting simulations produce noticeably poorer fits to the data. It is not possible to simulate the data with a single species. The simulations of the two species that are summed to give the resulting X-band fit to the data are shown in Figure 7C and D. The total concentration of the NO species agrees with the heme concentration of the protein, indicating quantitative conversion to the NO bound states of the hemes. Species r1-NO shows a three line pattern with hyperfine tensor $\mathbf{A}$ = (48, 49, 39) MHz from the ^{14}N nuclei ($I = 1$) of NO. The hyperfine parameters for species r2-NO cannot be determined due to its broad features; thus the *g*-strain in the simulation (see figure caption) is significantly larger than that of r1-NO, as it accounts for the unresolved hyperfine splitting.

Approximately 2 equiv of NO was also added to a reduced TDO EPR sample, which contained 10 equiv of L-Trp. A rhombic $S = 1/2$ EPR signal is observed with a resolved 9-line hyperfine pattern at g_{mid} for X-band (Figure 8A) and unresolved for Q-band (Figure 8E). Spectra B and F of Figure 8 show simultaneous least-squares fits of X- and Q-band spectra, respectively, which again require two species. The simulations are the sum of two species (r1-Trp-NO, r2-Trp-NO) in equal amounts using the parameters given in Table 1. The individual species simulations are shown in Figure 8C and D. Each species has changed from that in the absence of L-Trp. The total concentration of the NO species agrees with the heme concentration of the protein, indicating quantitative conversion to the NO bound states of the hemes. Species r1-Trp-NO displays a 9-line hyperfine pattern at $g_{mid} = 2.005$, which is a triplet of triplets with a smaller hyperfine constant ($A = 21$ MHz) originating from ^{14}N of the axial His, and a larger hyperfine constant ($A_{iso} = 43$ MHz) from ^{14}N of NO axial to the iron. The second NO adduct (r2-Trp-NO) does not show a resolved hyperfine pattern. These EPR signals are similar to those observed from the NO adducts of horse radish peroxidase (HRP) and hemoglobin (Hb).[29–31] The peak at $g = 2.03$ in the Q-band spectrum (Figure 8E) is believed to be distorted by a rapid passage condition of the signal from r2-Trp-NO, and thus an inaccurate simulation. Attempts to detect a nonpassage signal at higher temperatures were unsuccessful due to low signal-to-noise.

In the course of the NO experiments and simulations that identified the two species in these samples, it was noticed that the intensity ratio of the peaks at g = 2.093 and 2.046 in Figure 8A changed for some samples. The sample of the NO adduct of TDO with L-Trp was exposed to white light from a 300 W tungsten lamp for 5 min while at 77 K in the EPR tube. The EPR spectra before and after exposure to light are shown in Figure 9A and B, and the difference spectrum is Figure 9D. The spectrum after light exposure matches the simulation of species r1-Trp-NO from Figure 8C, which is repeated in Figure 9C. Also, the difference spectrum matches species r2-Trp-NO from Figure 8D, which is repeated in Figure 9E, indicating that the signal from the species r2-Trp-NO is lost due to photodissociation. It is worth noting that the simulations shown in Figure 8 were determined from least-squares fits to the spectra prior to the discovery of light sensitivity of one of the NO adducts. Thus, the photodissociation experiments confirm the validity of the least-squares fits to the experimental spectra of Figure 8.

Upon anaerobic thawing and refreezing of the sample in the dark, the before light spectrum is fully recovered (Figure 9F). Subsequent experiments showed that the same sample could by repeatedly cycled to produce on and off states of NO by photodissociation. Similar experiments were performed on a Q-band sample. Spectra G and H in Figure 9 show the spectra before and after exposure to light. Figure 9I shows that the Q-band simulation for species r1-Trp-NO matches the after light spectrum, which is in agreement with the X-band results. These light exposure experiments were also performed on samples of the NO adduct without L-Trp. The spectra of the samples without L-Trp did not change after exposure to light.

For all of the above NO samples and the photodissociation experiments, there is no evidence for the presence of the minority species that were observed in the oxidized and reduced states of TDO in the absence of NO. Either the 10% minority species are not resolved from the majority species, or the minority species are not present for the NO adducts.

The addition of NO (from NONOate donor) to the Mössbauer sample of reduced TDO in the presence of L-Trp is shown in Figure 10A. The spectrum shows the formation of new species and loss of all reduced TDO species, indicating complete binding of NO to all iron sites. This spectrum resembles that of the S = 1/2 NO-adduct of hemoglobin observed previously.[32] Simulations are not presented due to two species that have large anisotropy in the A-tensors. The Mössbauer sample was exposed to white light for 1 h at 77 K, and the resulting spectrum is shown in Figure 10B. A quadrupole doublet appears with parameters of δ = 0.95 mm/s, ΔE_Q = 2.54 mm/s for 15% of the total iron in the sample. These parameters are the same as the high-spin ferrous heme species from reduced TDO in the presence of L-Trp (r2-Trp). The relatively small amount of photolysis observed from Mössbauer as compared to EPR is due to the higher concentration of the Mössbauer samples, and to the opaqueness of the sample holder. The specific change to r2-Trp-NO due to photodissociation of NO allows correlation of the species r1 and r2 between EPR and Mössbauer data as discussed below.

Discussion

TDO has been isolated and characterized from *Pseudomonas*,[23,24,33,34] *Ralstonia metallidurans*,[14] *Xanthomonas campestris*,[13,22] human,[17–20] and rat liver.[10,12,23,24,33,35] The enzyme is a homotetramer in all characterized sources, and human TDO has considerable homology with bacterial TDO.[13] Three crystal structures of wild-type TDO have been published: the oxidized state without L-Trp from *Ralstonia metallidurans* and *Xanthomonas campestris*, and the reduced state with L-Trp from *Xanthomonas campestris*.[13,14] All of these structures indicate a dimer of dimer quaternary structure for the protein, where the active site of one monomer contains side chain groups from a second monomer. The spectroscopic data presented here from *Ralstonia metallidurans* support this dimer of dimer configuration of TDO and extend it to the electronic properties of the hemes. In the ensuing discussion, the two different protein monomers within each dimer will be referred to as monomers 1 and 2. The oxidized and reduced states of tetrameric TDO will use labels o and r. In all experiments, except for cryoreduction, the labeling of the oxidation states of the hemes and the protein state are synonymous. The discussion begins with the O_2 surrogate adducts of reduced TDO, as it presents the clearest evidence for the presence of equimolar amounts of two electronically inequivalent hemes.

O_2 Surrogates Bound to the Reduced State of TDO

The EPR and Mössbauer data from multiple samples of reduced TDO in the presence of NO or CO, independent of L-Trp, show two inequivalent heme sites in equal amounts. The addition of NO to reduced TDO generates two electronically inequivalent heme–NO adducts (r1-NO, r2-NO) in equal amounts, both of which are $S = 1/2$ [Fe(II)–NO][7] heme complexes. Previous studies have shown that the coordination number of the heme–NO species is correlated to the orientation of *g*-tensors and magnitude of *g*-values.[36,37] Five-coordinate heme–NO species have g_{min} oriented near to the Fe–NO bond axis, resulting in stronger hyperfine constant along g_{min} and a value close to 2.0, whereas for 6-coordinate species, the value of g_{min} is below 2.0 and off axis. The *g*-tensors for various heme–NO complexes are given in Table 3. The correlation of *g*-values between the NO adducts of TDO and those listed in Table 3 indicates that r1-NO and r2-NO species are 5- and 6-coordinate heme–NO adducts, respectively, as shown in Figure 11, with the loss of the bond to the proximal His240 for r1-NO. The proximal and distal histidines residues are 240 and 55 (*Xanthomonas campestris*), or 257 and 72 (*Ralstonia metallidurans*), respectively. Although the present work is from *Ralstonia metallidurans*, the residue numbering used throughout this Article is based on TDO from *Xanthomonas campestris*,[13] because structures are available for both oxidized and reduced states.

The binding of NO to reduced TDO in the presence of L-Trp also generates two electronically inequivalent $S = 1/2$ heme–NO adducts (r1-Trp-NO, r2-Trp-NO) in equal concentration, both of which are electronically different from the species observed without L-Trp. The *g*-values of the species with L-Trp indicate that they are both 6-coordinate. Thus, in the presence of L-Trp, r1 retains the His240 bond. Consistent with the presence of this bond, species r1-Trp-NO displays a 9-line triplet of triplets pattern that resembles the NO–heme–His complex of HRP.[29] The broader unresolved spectrum of r2-Trp-NO is rare, but

has been observed for Hb.[30,31] The correlation between the NO adducts with and without L-Trp of the two species is based on the observation of resolved ^{14}NO hyperfine in the signals from r1-NO and r1-Trp-NO, whereas the signals from r2-NO and r2-Trp-NO do not show resolved hyperfine.

These EPR spectra are similar to previously published spectra of TDO from *Pseudomonas*.[34] This previous work was unaware of heme species differences in the tetramer of TDO, but it is clear from the present work, and the similarity of spectra, that the older spectra of TDO from *Pseudomonas* contain two NO species, similar to that of *Ralstonia metallidurans*. Recent resonance Raman studies of human TDO have identified only a single NO species from human TDO.[17] Presumably, the second species is not evident in the resonance Raman spectra due to overlapping signals, or possibly the hemes are more equivalent for human TDO.

Exposure of the NO adduct of TDO-Trp to light at 77 K resulted in loss of the EPR signal from r2-Trp-NO, without change to the signal from r1-Trp-NO, and the generation of a ferrous heme quadrupole doublet with $\Delta E_Q = 2.54$ in Mössbauer spectroscopy. This result provides a basis for the labeling of the two heme species in TDO with and without NO. The loss of NO from r2-Trp-NO gives a quadrupole doublet, which is identified in the reduced TDO Mössbauer as the r2-Trp state. Upon warming the sample, the r2-Trp-NO species is regenerated, and this loss and gain of NO to r2-Trp is reproducible in the same sample. The stabilization of the r2-Trp state after photolysis of r2-Trp-NO implies that the NO molecule moves out of the O_2-substrate site. In contrast, in the absence of L-Trp (r1-NO, r2-NO), or for one site with L-Trp (r1-Trp-NO), the NO is confined to the substrate pocket. Presumably photolysis does occur, but with immediate rebinding. Such geminate recombination of photolyzed adducts is well-known from studies of Mb-CO.[38] The motion of NO implies that the protein monomer of r2-Trp has a substrate site with a more open configuration than the monomers for the states r1, r2, or r1-Trp. This may have functional significance for TDO, suggesting that access of O_2 to the substrate site is favored for one site over the other site.

Upon addition of CO to reduced TDO or TDO-Trp, all species in the Mössbauer spectra convert to an equal mixture of two species with parameters given in Table 2. The Mössbauer parameters of these species are typical of the diamagnetic CO adduct of ferrous heme complexes.[28] The difference in the quadrupole splitting is presumably correlated to the protonation state of His240, but, at present, it is not possible to determine which species is associated with site 1 or 2.

Oxidized State of TDO

In the presence of L-Trp, both EPR and Mössbauer data show two major species (o1-Trp-OH, o2-Trp) in unequal amounts. This speciation is not immediately evident for oxidized TDO without Trp; however, both the EPR and the Mössbauer spectrum are compatible with the presence of two species with D and E/D values in the range $10 < D < 15$ cm^{-1} and $0.005 < E/D < 0.01$. Furthermore, the cryoreduction of oxidized TDO clearly shows the presence of two inequivalent heme species in equal amounts, indicating that the inequivalency of heme sites might not necessarily be exclusively dependent on L-Trp.

At pH 6.0, in the absence of L-Trp, the EPR spectrum of oxidized TDO converts to a signal that is identical to that of the high-spin species in the presence of L-Trp (o2-Trp). The addition of L-Trp at low pH does not result in the formation of the Fe(III)–OH species. Together, these two results imply that acidic conditions cause heme o1 to convert to a species that is electronically equivalent to heme o2. Under basic conditions (pH 8.4), the EPR signals of TDO and TDO-Trp are the same as that at neutral pH. The neutral pH EPR spectrum can be decomposed into two species of equal amounts, a more rhombic species (o1, E/D = 0.010) and a more axial species (o2, E/D = 0.006), to give an equally good fit to the experimental spectrum as that shown in Figure 1 for a single species.

These results indicate a different relationship between the monomeric subunits of TDO from *Ralstonia metallidurans* as compared to previous studies of TDO from rat liver or *Pseudomonas*.[23,24,33] The predominant explanation for the existence of the two species in oxidized TDO has been an acid–alkaline heme transition that is pH and L-Trp dependent. In previous studies, a single acid–alkaline transition was observed from pH 6.6 to 9.0 for the tetrameric protein and described by a single pK_a value, which shifted downward in the presence of L-Trp.[33] Our findings suggest an alternative explanation in which TDO contains two electronically inequivalent heme sites and only one of these sites can be titrated in this pH range. The crystal structure of reduced TDO-Trp shows H-bonds between the distal side water and to both His55 and L-Trp for one monomer, whereas the other monomer has no H-bonds to water.[13] If His55 and L-Trp are also closer for site 1 of oxidized TDO with L-Trp, H-bonds formed in the presence of L-Trp may stabilize the OH^- adduct as suggested in Figure 12. The axially coordinated water is based on previous studies.[14,17,23] The aquo/hydroxo transition in TDO with L-Trp occurs at approximately 2 pH units lower than that of sperm whale myoglobin (pK_a 8.939). While both proteins have a distal His that can provide a H-bond to stabilize the hydroxo adduct, it may be that the lower pK_a for this conversion in TDO is a consequence of an additional H-bond to L-Trp. However, the reduction potential of TDO with L-Trp (+130 mV[13]) is more positive than sperm whale myoglobin (+20 mV[40]), indicating that the protein environment of the heme also contributes to the pK_a drop of TDO relative to myoglobin.

Reduced State of TDO

The interpretation of the Mössbauer spectra of reduced TDO in the absence of O_2 surrogates is complicated by the overlap of doublets; however, the spectra show at least two inequivalent ferrous high-spin heme species with lower and higher quadrupole splittings of ΔE_Q = 3.3 mm/s (species r1) and ΔE_Q = 3.8 (species r2), accounting for 80% of the iron. In the presence of L-Trp, a new high-spin ferrous heme species is observed with a significantly smaller value of ΔE_Q = 2.54 mm/s (species r2-Trp). These species assignments are corroborated by the cryoreduction and photodissociation results. Thawing of the cryoreduced sample of TDO causes the quadrupole splitting of one species to change from 2.54 to 3.8 mm/s, consistent with assignment to r2. Photodissociation of NO from one of the sites (r2-Trp-NO) gives a species (r2-Trp) with quadrupole splitting of 2.54 mm/s. The concentrations of the two species are consistent between the oxidized and reduced states of TDO in the presence of L-Trp: 35% (site 1) and 45% (site 2). Presumably, the concentrations of the two sites are unequal due to heterogeneity in the protein and presence

of the minor species. In the presence of the O_2 surrogates, or for cryoreduction in the absence of L-Trp, the concentrations of the two sites are observed to be equal.

Independent of the species assignments, it is clear that at least one of the major species undergoes a significant change in its electronic properties upon binding of L-Trp. The lower value of ΔE_Q = 2.54 mm/s is in the range of other heme proteins with an axial His ligand from the protein: Mb (–2.22 mm/s), Hb (–2.40 mm/s), HRP (+2.68 mm/s).[28] The higher ΔE_Q values, 3.3–3.8 mm/s, are rare in proteins, but larger values have been observed in the heme enzyme hydroxylamine oxidoreductase (4.21 mm/s).[41] Recent studies of ferrous porphyrins have shown a strong correlation between the value of ΔE_Q and the protonation state of the N_δ-imidazole.[15,42–44] For neutral imidazole, similar to Mb and Hb, the values of ΔE_Q are negative, $-2.4 < \Delta E_Q < -1.9$, whereas for negative imidazolate (deprotonated N_δ), the values are positive and larger in magnitude, $+2.6 < \Delta E_Q < +3.8$. H-bonding interactions to the proximal histidine in proteins (e.g., HRP[45]) can induce imidazolate-like character, thereby changing the sign from negative to positive. The signs of ΔE_Q could not be determined for the hemes of TDO due to the mixture of species; nevertheless, the large change in the magnitude of ΔE_Q upon L-Trp addition indicates a change in the electronic character of His240-N_δ of TDO. The large values of ΔE_Q (without L-Trp) indicate significant imidazolate character for His240, whereas the smaller value of ΔE_Q (with L-Trp) indicates more imidazole character. The change in the structure need not necessarily be from pure imidazole to pure imidazolate, because the effect could be mitigated by H-bonds to His240: weaker H-bonding for imidazole-like, stronger H-bonding for imidazolate-like.

In a recent resonance Raman study of human TDO, the spectra of reduced enzyme were interpreted as a single species with an Fe-His vibration that is not affected by the presence of L-Trp.[17] In addition, the Fe-His vibration frequency was between that of globins and peroxidases. This suggests that the monomers of TDO from *Ralstonia metallidurans* and human may not exhibit the same quaternary interactions as they extend to the electronic properties of the hemes of TDO. We note, however, that the oxidized states of both *Ralstonia metallidurans* and human TDO with L-Trp show the simultaneous presence of high-and low-spin ferric species in roughly the same ratio of amounts. As stated above, the effect of L-Trp on oxidized TDO is attributed to the low-spin conversion of only one heme site. Thus, the presence of these two species in human TDO suggests that the heme inequivalency is also present in human TDO.

The crystal structure of reduced TDO with L-Trp from *Xanthomonas campestris* shows differences between the two monomers at the distal water near the L-Trp and His55, but this water has no axial interaction with the hemes.[13] The proximal His240 is H-bonded via N_δ to a string of two waters leading to Tyr, but the structures of the two monomers are essentially the same at His240, with no apparent differences in H-bonds. This part of the structure does not appear to be compatible with the frozen solution Mössbauer data that show species with significantly different quadrupole splitting values. It is expected that differences in the protonation state of His240, which are sufficient to produce the observed different quadrupole splittings of the species, should also be apparent in the crystal structure. The structures for the reduced states of TDO from *Ralstonia metallidurans* are not available; possibly the structures of the enzymes from *Ralstonia metallidurans* and *Xanthomonas*

campestris are not equivalent. When a structure of reduced TDO without L-Trp becomes available, it is expected that this structure will show significant changes in the H-bonding interactions to His240 relative to that of the structure with L-Trp.

Cryoreduction of Oxidized TDO

Cryoreduction of oxidized TDO produces two new species in Mössbauer spectra in equal amounts. The protein remains frozen during reduction and thus retains the overall conformation of the oxidized tetramer, indicating that oxidized TDO contains two electronically inequivalent heme sites.

One of the species observed after cryoreduction is a novel heme state (δ = 0.55 mm/s, ΔE_Q = 1.70 mm/s). It is clearly a diamagnetic species and must therefore be in the ferrous oxidation state. The values of δ and ΔE_Q are not typical of known low-spin hemes: $0.30 < \delta < 0.45$ mm/s, $\Delta E_Q < 1.5$ mm/s.[27] A literature search did not find other ferrous heme proteins or porphyrin complexes with Mössbauer parameters similar to the new species. The new species is tentatively assigned as the hydroxy adduct His-heme(Fe^{2+})-OH of site 1 ($o1^{red}$-OH), which would be a reduced form of the hydroxy complex observed from site 1. The correlation to site 1 is based on the hydroxy adduct of oxidize TDO and the results following sample annealing. Other conceivable ligands that might give a low-spin species are O_2 and His55. However, O_2 is ruled out because its solution concentration is insufficient to give the amount detected, and the isomer shifts for oxy-heme species are much lower, $\delta \approx 0.27$ mm/s.[28] Coordination of His55 is also ruled out because the distance of N_δ-His55 from iron is 5.2 Å,[14] and the Mössbauer parameters are not in the range of bis-His heme species.

For the hydroxy adduct, the overall charge of the heme moiety is reduced by two upon photoreduction: $[PorFe^{3+}–OH_2]^{1+} + e^- \rightarrow [PorFe^{2+}–OH]^{1-} + H^+$. Figure 13 shows the assignments of species and a possible stabilization of the hydroxy adduct in site 1. It is suggested that the hydroxy adduct is stabilized by a combination of the proximal His240 with significant imidazole character and H-bond formation to His55. Upon annealing, the quadrupole splitting of $o1^{red}$-OH changes from 1.70 to 3.31 mm/s ($o1^{red}$-anneal), which is identified as one of the major species (r1) in reduced TDO, and thus $o1^{red}$-anneal is equated with r1. During the annealing, the protein relaxes to the reduced conformation of TDO. The change in the quadrupole splitting is attributed to proton transfers to the axial hydroxide and away from His240, thereby forming species r1, which is 5-coordinate high-spin ferrous with imidazolate character for His240. Thawing the sample under anaerobic conditions did not change the species, indicating a stable state of the protein.

The other of the two ferrous species observed after cryoreduction ($o2^{red}$) has a quadrupole doublet with ΔE_Q = 2.54 mm/s, indicating the generation of a site with the electronic properties similar to that of the r2-Trp state, but in the absence of Trp. This species does not change after annealing the sample. Upon thawing the sample, this site undergoes a shift in the quadrupole splitting from 2.5 to 3.8 mm/s, which is identified as the other major species in reduced TDO, and thus the correlation with species r2.

The cryoreduction result provides a basis for a correlation between the two heme sites in the oxidized and chemically reduced conformations of tetrameric TDO. For oxidized TDO, the

protein monomer of site 1 is capable of stabilizing lower charge states of the heme moiety relative to that of the protein monomer of site 2; thus site 1 stabilizes the hydroxy adduct o1-Trp-OH. The cryoreduced state of oxidized TDO also appears to produce a hydroxy adduct ($o1^{red}$-OH), which provides a basis for the correlation between site 1 of oxidized TDO. Upon annealing of the cryoreduced sample, the species $o1^{red}$-OH changes its quadrupole splitting 3.3 mm/s, which is identified as species r1 of reduced TDO, and thus the correlation with species o1 and r1. The other species in the cryoreduced sample ($o2^{red}$) undergoes a shift in the quadrupole splitting to 3.8 mm/s upon thawing the sample, and thus the correlation with species o2 and r2.

Proximal versus Distal Pocket Heme Effects

The crystal structures of TDO show a dimer of dimer quaternary structure and distinct differences in the protein structures near the substrate pocket between the two sites of a dimer. These site differences are most profound at the distal side of the substrate pocket. Thus, our finding of inequivalent hemes for the two sites is reasonable when the O_2 binding site (axial coordination to the heme) is occupied with NO or CO. In this case, the O_2 surrogate can interact through H-bonds with the structural elements of the distal pocket that are different for the two sites, and thereby convey a difference in electronic properties to the hemes of each site. These electronic differences are also evident in the presence of L-Trp, which renders one of the hemes low-spin with an axial hydroxide coordination to the Fe. In this case, the hydroxide is likely stabilized by distal pocket interactions, and thus, like the O_2 surrogates, distal pocket interactions are invoked as the origin of the heme site differences.

In the absence of the O_2 surrogates, the specific protein interactions with the hemes that cause the electronic differences are less clear. The reduced high-spin hemes are 5-coordinate and do not possess an axial ligand that could interact with the distal pocket. The Mössbauer quadrupole splitting values of the two sites for reduced TDO (r1, r2) are different, but both values are in the range 3.3–3.8 mm/s, consistent with both sites having more imidazolate-like character for the proximal His. This difference in magnitude could possibly be induced by more subtle effects, such as differences at the heme periphery. In the presence of L-Trp, however, the quadrupole splitting of site 2 changes significantly from 3.8 to 2.5 mm/s. The lower value (2.5 mm/s) is indicative of more imidazole-like character of the proximal His of site 2. These same quadrupole splittings are also observed in the cryoreduced sample in the absence of L-Trp. Thus, the dimer of dimer quaternary structure also has an effect on the proximal side, generating two sites with different protonation states of the proximal His. Direct interactions of heme with the protein from the distal side cannot be invoked because there is no axial heme ligand on the distal side.

Conclusions

Two electronically inequivalent heme sites are observed for TDO. This inequivalency is likely an extension of the dimer of dimer quaternary protein structure to the heme sites. In the presence of O_2 surrogates, the heme inequivalency could originate from interactions of the axial heme ligand with the distal protein pocket.

The protonation state of the proximal His changes in the presence of L-Trp. While we cannot rule out this protonation state change for both sites, the present data suggest that only one of the sites of each dimer undergoes this change.

The binding of O_2 surrogates NO or CO shows two inequivalent heme sites. The heme–NO complexes are 5- and 6-coordinate without L-Trp, and both 6-coordinate with L-Trp. NO can be photodissociated from only one of the heme–NO sites and only in the presence of L-Trp. The selective photodissociation of NO from the r2-Trp site implies that the substrate site of corresponding protein monomer has a more open path to the solvent, suggesting that access of O_2 to the substrate site is favored for one active site over the other.

The cryoreduction of TDO produces a novel diamagnetic reduced heme species, which is tentatively assigned to the formation of a His–heme(Fe^{2+})–OH protein complex. This work presents a new description of the heme interactions with the protein, and with the proximal His, that must be considered during the general interpretation of physical data as it relates to kinetics, mechanism, and function of TDO. The inequivalency of hemes has similarities to Hb, but interestingly, whereas the different hemes in Hb hemes are associated with its $\alpha_2\beta_2$ quaternary structure, TDO is a homotetramer. For dimeric enzymes that possess inequivalent functional sites in otherwise two similar protein monomers, a half-sites reaction mechanism has been invoked. The consequence of the inequivalence of hemes on the function of TDO, and if a half-sites reaction mechanism might apply for this tetrameric enzyme, are at present open questions.

Supplementary Material

Refer to Web version on PubMed Central for supplementary material.

Acknowledgments

This work is supported by NIH Grant GM077387 (M.P.H.) and NSF Grant MCB-0843537 (A.L.). R.F. acknowledges generous fellowship support from the Molecular Basis of Disease (MBD) program of Georgia State University.

References

1. Kurnasov O, Goral V, Colabroy K, Gerdes S, Anantha S, Osterman A, Begley TP. Chem Biol. 2003; 10:1195–1204. [PubMed: 14700627]
2. Stone TW, Darlington LG. Nat Rev Drug Discovery. 2002; 1:609–620.
3. Schwarcz R. Curr Opin Pharmacol. 2004; 4:12–17. [PubMed: 15018833]
4. Robotka H, Toldi J, Vcsei L. Future Neurol. 2008; 3:169–188.
5. Guillemin GJ, Meininger V, Brew BJ. Neurodegener Dis. 2005; 2:166–176. [PubMed: 16909022]
6. Guillemin GJ, Brew BJ. Redox Rep. 2002; 7:199–206. [PubMed: 12396664]
7. Yamamoto S, Hayaishi O. Methods Enzymol. 1970; 17:434–438.
8. Myint AM, Schwarz MJ, Steinbusch HWM, Leonard BE. Metab Brain Dis. 2009; 24:55–68. [PubMed: 19067144]
9. Reinhard JF Jr. Ann NY Acad Sci. 2004; 1035:335–349. [PubMed: 15681816]
10. Hillier J, Hillier JG, Redfern PH. Nature. 1975; 253:566–567. [PubMed: 1117992]
11. Kotake Y, Masayama I. Z Physiol Chem. 1936; 243:237–244.
12. Feigelson P, Greengard O. Biochim Biophys Acta. 1961; 50:200–202. [PubMed: 13698618]

13. Forouhar F. Proc Natl Acad Sci USA. 2007; 104:473–478. [PubMed: 17197414]
14. Zhang Y, Kang SA, Mukherjee T, Bale S, Crane BR, Begley TP, Ealick SE. Biochemistry. 2007; 46:145–155. [PubMed: 17198384]
15. Sugimoto H, Oda S, Otsuki T, Hino T, Yoshida T, Shiro Y. Proc Natl Acad Sci USA. 2006; 103:2611–2616. [PubMed: 16477023]
16. Thackray SJ, Mowat CG, Chapman SK. Biochem Soc Trans. 2008; 36:1120–1123. [PubMed: 19021508]
17. Batabyal D, Yeh SR. J Am Chem Soc. 2007; 129:15690–15701. [PubMed: 18027945]
18. Chauhan N, Basran J, Efimov I, Svistunenko DA, Seward HE, Moody PCE, Raven EL. Biochemistry. 2008; 47:4761–4769. [PubMed: 18370410]
19. Basran J, Rafice SA, Chauhan N, Efimov I, Cheesman MR, Ghamsari L, Raven EL. Biochemistry. 2008; 47:4752–4760. [PubMed: 18370401]
20. Batabyal D, Yeh SR. J Am Chem Soc. 2009; 131:3260–3270. [PubMed: 19209904]
21. Papadopoulou ND, Mewies M, McLean KJ, Seward HE, Svistunenko DA, Munro AW, Raven EL. Biochemistry. 2005; 44:14318–14328. [PubMed: 16245948]
22. Thackray SJ, Bruckmann C, Anderson JLR, Campbell LP, Xiao R, Zhao L, Mowat CG, Forouhar F, Tong L, Chapman SK. Biochemistry. 2008; 47:10677–10684. [PubMed: 18783250]
23. Uchida K, Shimizu T, Makino R, Sakaguchi K, Iizuka T, Ishimura Y, Nozawa T, Hatano M. J Biol Chem. 1983; 258:2519–2525. [PubMed: 6600455]
24. Uchida K, Shimizu T, Makino R, Sakaguchi K, Iizuka T, Ishimura Y, Nozawa T, Hatano M. J Biol Chem. 1983; 258:2526–2533. [PubMed: 6600456]
25. Petasis DT, Hendrich MP. J Magn Reson. 1999; 136:200–206. [PubMed: 9986761]
26. Golombek AP, Hendrich MP. J Magn Reson. 2003; 165:33–48. [PubMed: 14568515]
27. Que, L., Jr, editor. Physical Methods in Bioinorganic Chemistry: Spectroscopy and Magnetism. 2000. p. 556
28. Debrunner PG. Phys Bioinorg Chem Ser. 1989; 4:137–234.
29. Yonetani T, Yamamoto H, Erman JE, Leigh JSJ, Reed GH. J Biol Chem. 1972; 247:2447–2455. [PubMed: 4336375]
30. Huttermann J, Burgard C, Kappl R. J Chem Soc, Faraday Trans. 1994; 90:3077–87.
31. Hille R, Olson JS, Palmer G. J Biol Chem. 1979; 254:12110–20. [PubMed: 40990]
32. Oosterhuis WT, Lang G. J Chem Phys. 1969; 50:4381–7.
33. Makino R, Sakaguchi K, Iizuka T, Ishimura Y. J Biol Chem. 1980; 255:11883–11891. [PubMed: 6254984]
34. Henry Y, Ishunura Y, Peisach J. J Biol Chem. 1976; 251:1578–1581. [PubMed: 176157]
35. Ren S, Liu H, Licad E, Correia MA. Arch Biochem Biophys. 1996; 333:96–102. [PubMed: 8806758]
36. Praneeth VKK, Neese F, Lehnert N. Inorg Chem. 2005; 44:2570–2572. [PubMed: 15819537]
37. Praneeth VKK, Nather C, Peters G, Lehnert N. Inorg Chem. 2006; 45:2795–2811. [PubMed: 16562937]
38. Austin RH, Beeson KW, Eisenstein L, Frauenfelder H, Gunsalus IC. Biochemistry. 1975; 14:5355–5373. [PubMed: 1191643]
39. Iizuka T, Morishima I. Biochim Biophys Acta. 1975; 400:143–53. [PubMed: 238653]
40. Taboy CH, Faulkner KM, Kraiter D, Bonaventura C, Crumbliss AL. J Biol Chem. 2000; 275:39048–54. [PubMed: 10984477]
41. Andersson KK, Kent TA, Lipscomb JD, Hooper AB, Munck E. J Biol Chem. 1984; 259:6833–40. [PubMed: 6327697]
42. Hu C, Noll BC, Piccoli PMB, Schultz AJ, Schulz CE, Scheidt WR. J Am Chem Soc. 2008; 130:3127–3136. [PubMed: 18271587]
43. Hu C, Roth A, Ellison MK, An J, Ellis CM, Schulz CE, Scheidt WR. J Am Chem Soc. 2005; 127:5675–5688. [PubMed: 15826208]
44. Hu C, Noll BC, Schulz CE, Scheidt WR. J Am Chem Soc. 2005; 127:15018–15019. [PubMed: 16248628]

45. Berglund GI, Carlsson GH, Smith AT, Szöke H, Henriksen A, Hajdu J. Nature. 2002; 417:463–467. [PubMed: 12024218]
46. Twigg AI, Baniulis D, Cramer WA, Hendrich MP. J Am Chem Soc. 2009; 131:12536–12537. [PubMed: 19689132]
47. Usov OM, Choi PST, Shapleigh JP, Scholes CP. J Am Chem Soc. 2006; 128:5021–5032. [PubMed: 16608336]
48. Derbyshire ER, Gunn A, Ibrahim M, Spiro TG, Britt RD, Marletta MA. Biochemistry. 2008; 47:3892–3899. [PubMed: 18302323]
49. Hayes RG, Ellison MK, Scheidt WR. Inorg Chem. 2000; 39:3665–3668. [PubMed: 11196830]
50. Wayland BB, Olson LW. J Am Chem Soc. 1974; 96:6037–41. [PubMed: 4415859]
51. LoBrutto R, Wei YH, Mascarenhas R, Scholes CP, King TE. J Biol Chem. 1983; 258:7437–48. [PubMed: 6305941]
52. O'Keeffe DH, Ebel RE, Peterson JA. J Biol Chem. 1978; 253:3509–16. [PubMed: 206545]

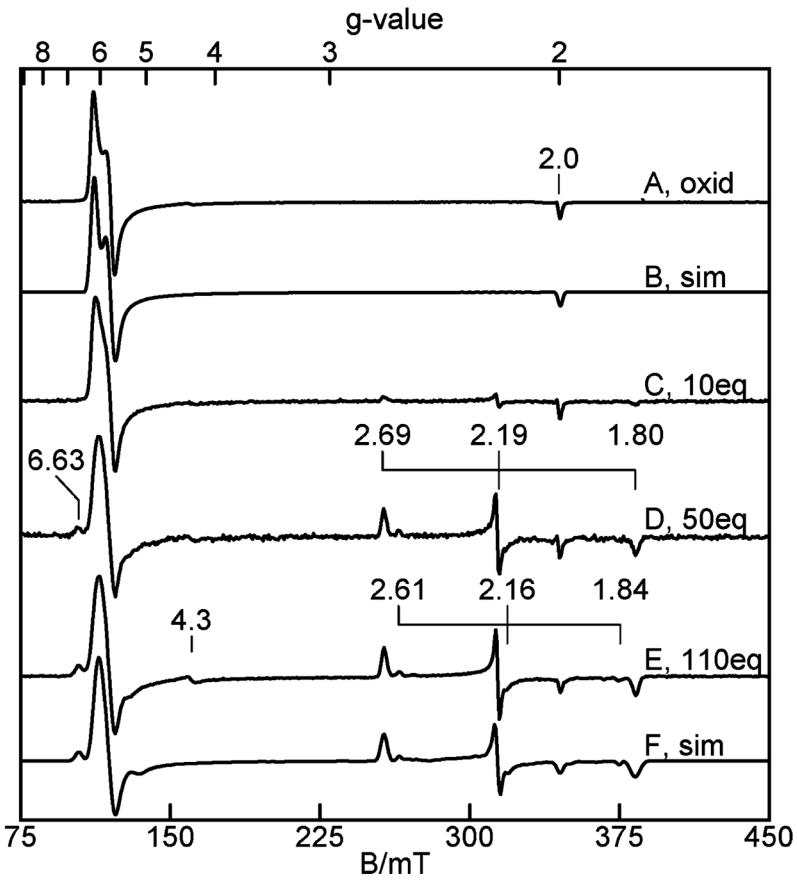

Figure 1.

EPR spectra of 220 μM oxidized TDO, pH 7.4. (A) As-isolated, (B) simulation of (A), (C) with 10 equiv of L-Trp, (D) with 50 equiv of L-Trp, (E) with 110 equiv of L-Trp, and (F) simulation of (E). Experimental conditions: microwaves, 0.2 mW at 9.65 GHz; temperature, 11 K. See text and Table 1 for simulation parameters.

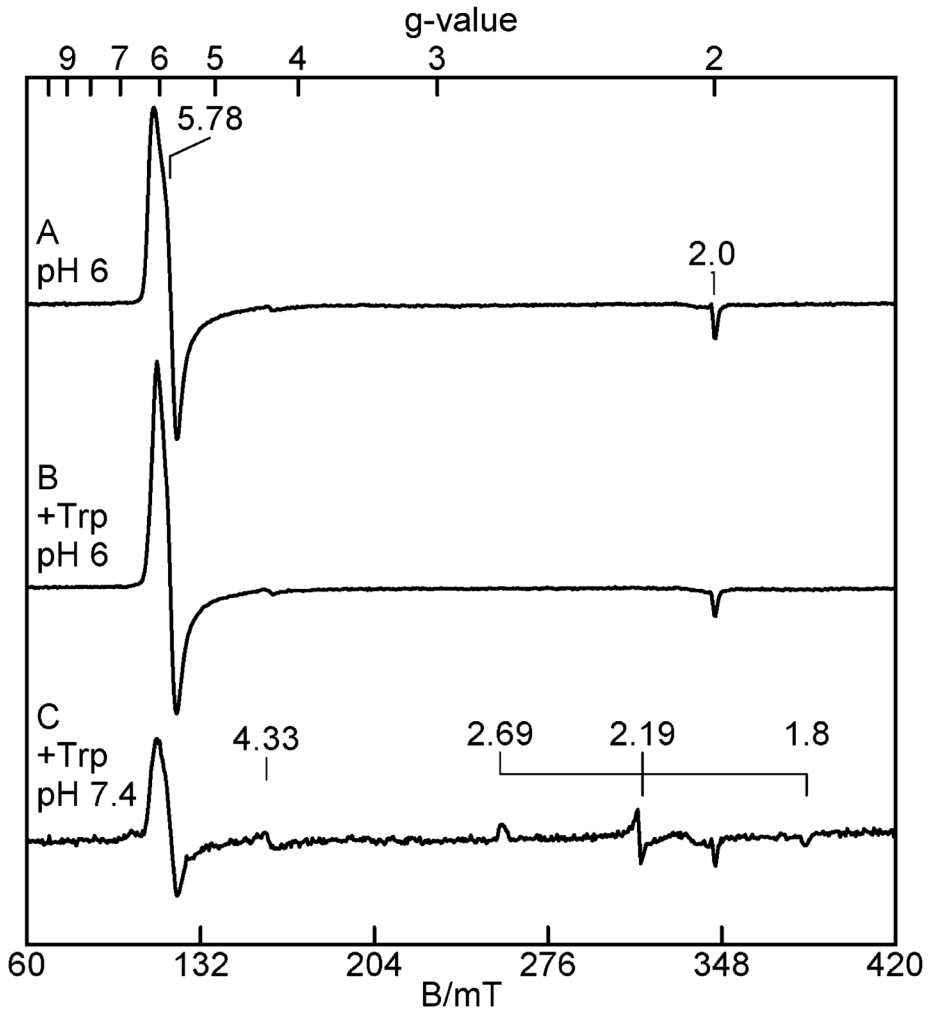

Figure 2.

EPR spectra of 115 μM oxidized TDO. (A) In 50 mM MES pH 6.0, 10% glycerol; (B) pH 6.0 with 50 equiv of L-Trp; (C) after buffer exchange to 50 mM Tris-HCl pH 7.4, 10% glycerol. Experimental conditions are the same as in Figure 1.

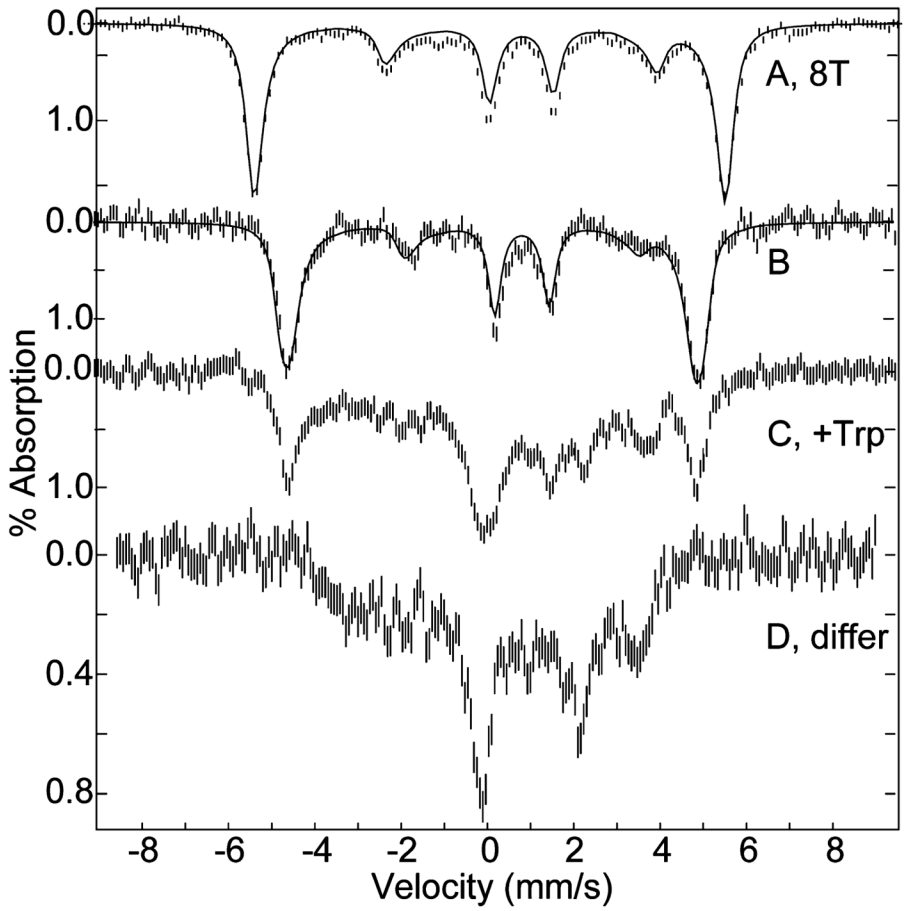

Figure 3.

Mössbauer spectra of 1 mM oxidized TDO, pH 7.4. (A) Oxidized TDO in a magnetic field of 8 T, (B) oxidized TDO, (C) with L-Trp, (D) difference spectrum of (C) – 0.4 (B). Experimental conditions: temperature, 4.2 K; magnetic field of 45 mT (except (A)) parallel to γ-ray direction. The solid lines are least-squares fits with parameters given in the text.

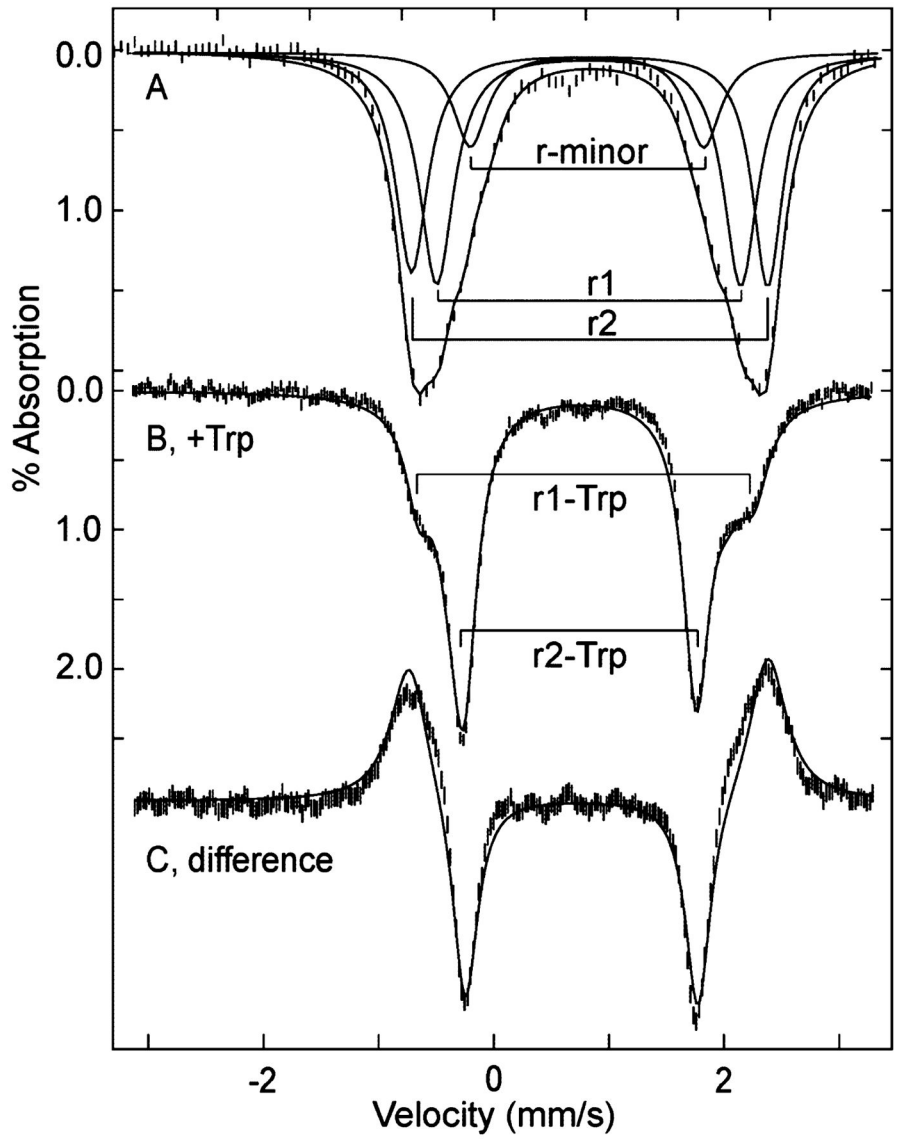

Figure 4.

Mössbauer spectrum of 1 mM TDO, pH 7.4. (A) Reduced, (B) reduced with 10 equiv of L-Trp, (C) difference spectrum (B)–(A) for equal areas of (A) and (B). All spectra recorded at 4.2 K in a magnetic field of 45 mT parallel to γ-ray direction. The solid lines overlaid on the data are least-squares fits using the parameters given in Table 2. The additional lines in (A) show the doublets of the individual species.

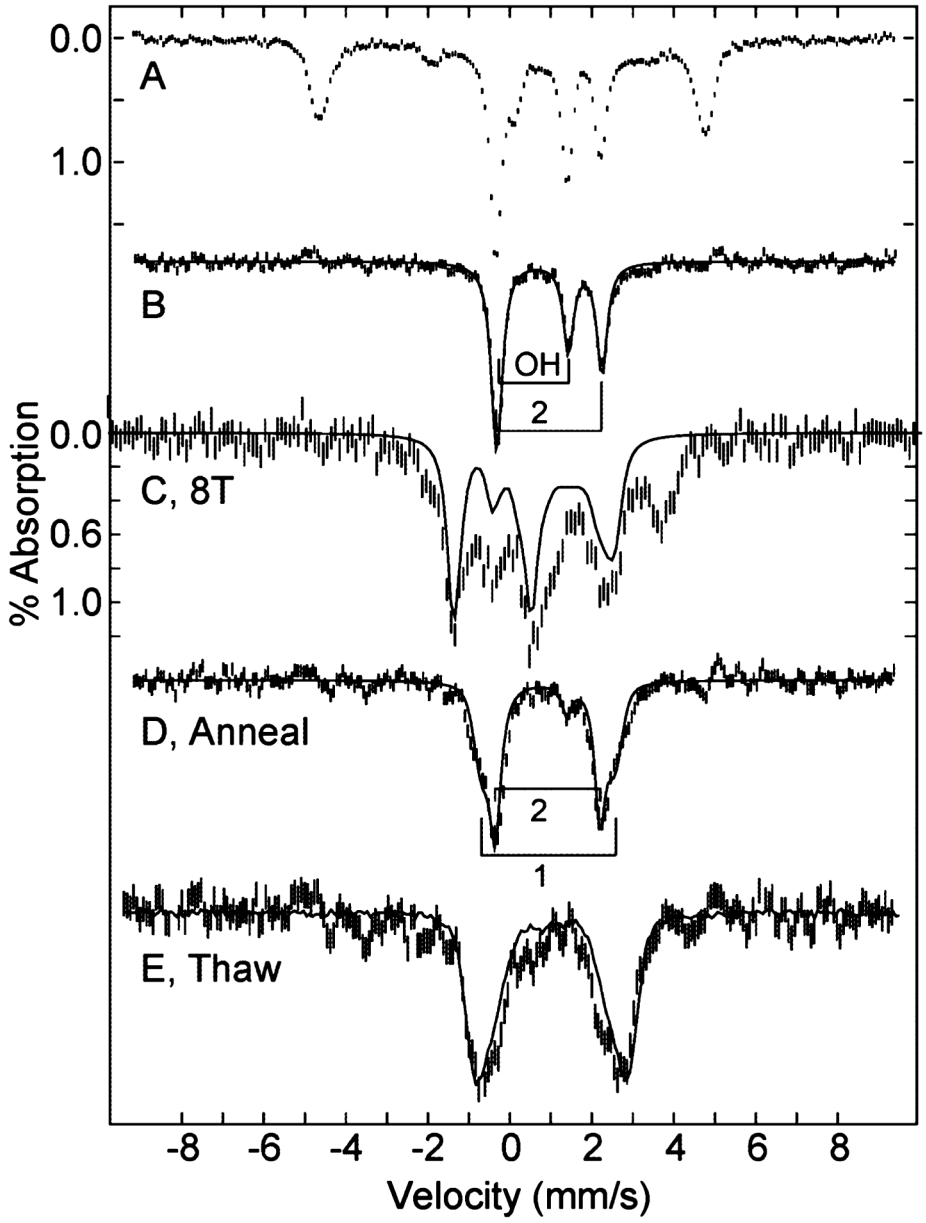

Figure 5.

Mössbauer spectrum after cryoreduction of (A) 1.5 mM oxidized TDO, pH 7.4. The difference spectra (B–E) after subtracting the spectrum of oxidized TDO are: (B) 45 mT; (C) 8 T; (D) after annealing; (E) after thawing, including an overlay (solid line) of the reduced TDO spectrum. All spectra are recorded at 4.2 K and magnetic field of 45 mT parallel to γ-ray direction, except (C). The solid lines in (B) and (D) are least-squares fits for species: (B) $o1^{red}$-OH (OH), $o2^{red}$ (2); and (D) $o1^{red}$-anneal (1), $o2^{red}$-anneal (2). The solid line in (C) is a simulation at 8 T for the $S = 0$ species $o1^{red}$-OH. See Table 2 for parameter listings of species.

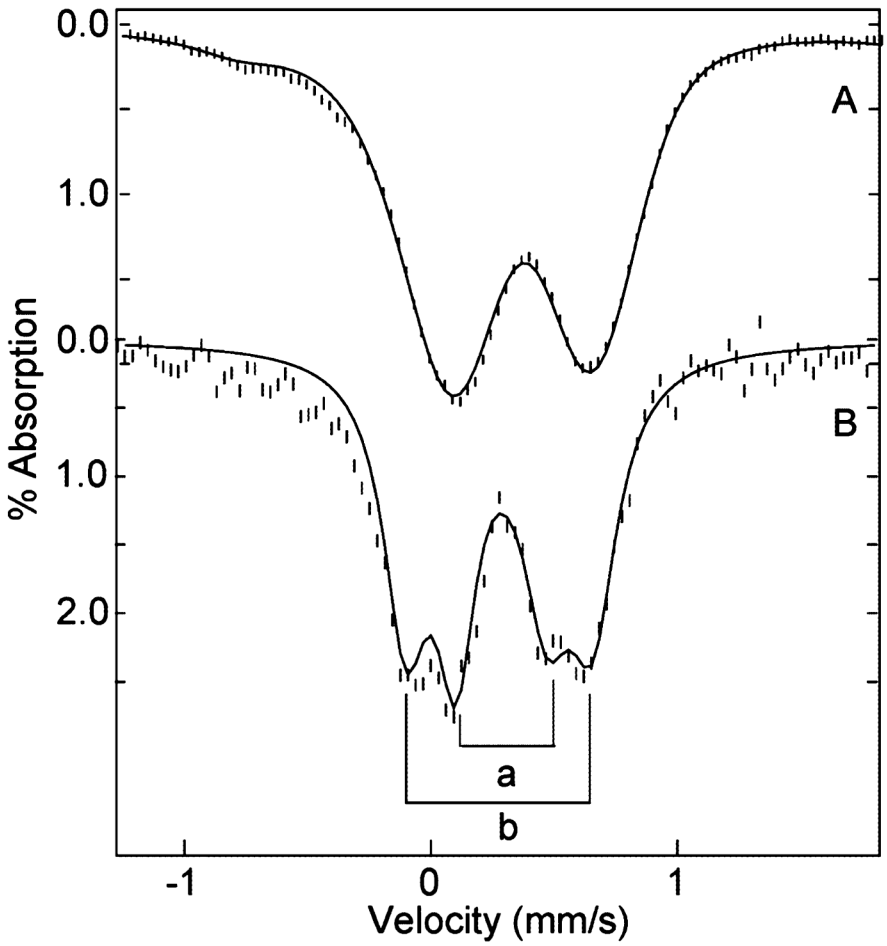

Figure 6.

Mössbauer spectrum of (A) 1.5 mM ferrous TDO, pH 7.4, with 10 equiv of L-Trp and excess CO; (B) Fourier transform of spectrum A with removal of intrinsic ^{57}Fe source line width. All spectra recorded at 4.2 K in a magnetic field of 45 mT parallel to γ-ray direction. The solid lines are least-squares fits using the parameters given in Table 2 for r_a-CO and r_b-CO.

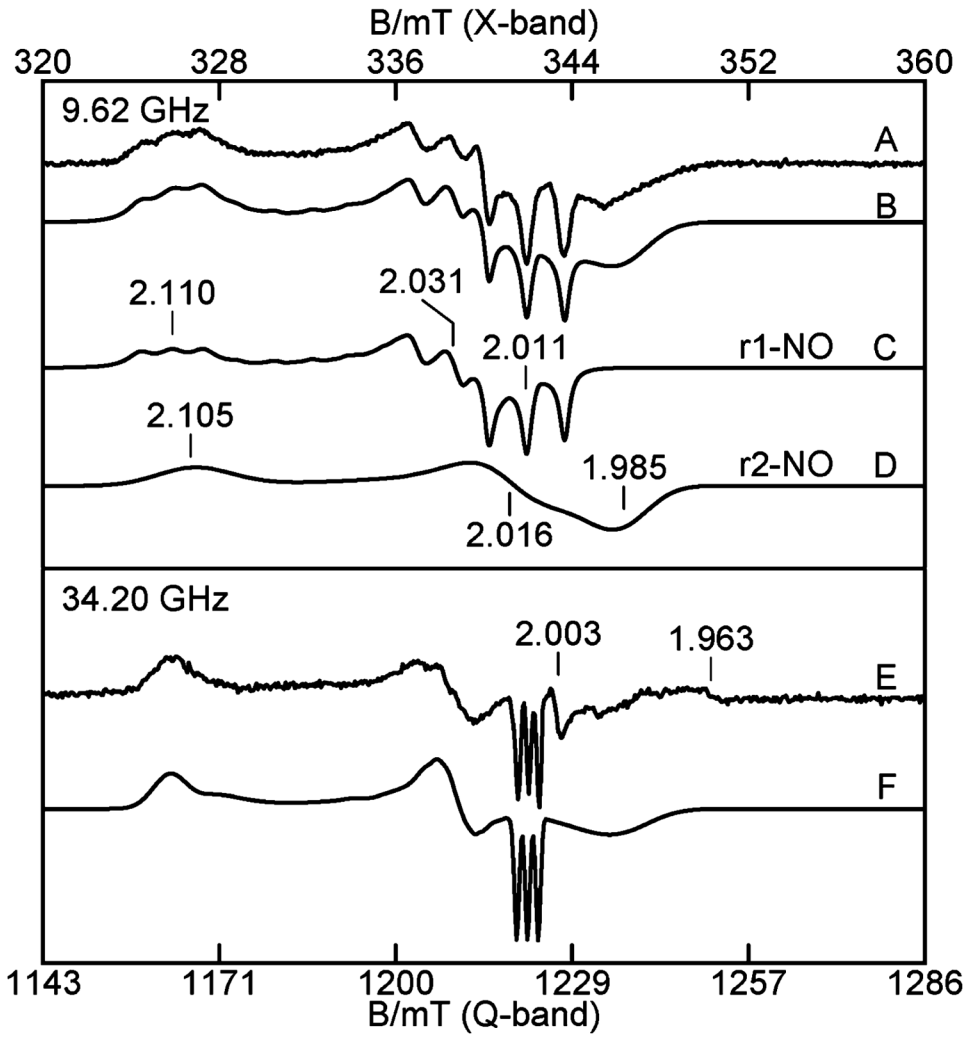

Figure 7.

(A) X- and (E) Q-band EPR spectra of the NO adduct of 0.3 mM reduced TDO without L-Trp. (B) Simulation sum (C) + (D) of the two sites, (C) simulation of r1-NO, (D) simulation of r2-NO, and (F) simulation sum of the two sites of (E). Experimental conditions: microwave frequencies as listed; power, 0.02 mW (X), 0.005 mW (Q); temperature, 20 K (X), 27 K (Q). The simulation parameters are given in Table 1, and σ_{g1} = (0.0015, 0.0032, 0.0044), σ_{g2} = (0.0074, 0.0089, 0.0107). The weak signal near g = 1.96 is due to a minor amount of free NO in solution.

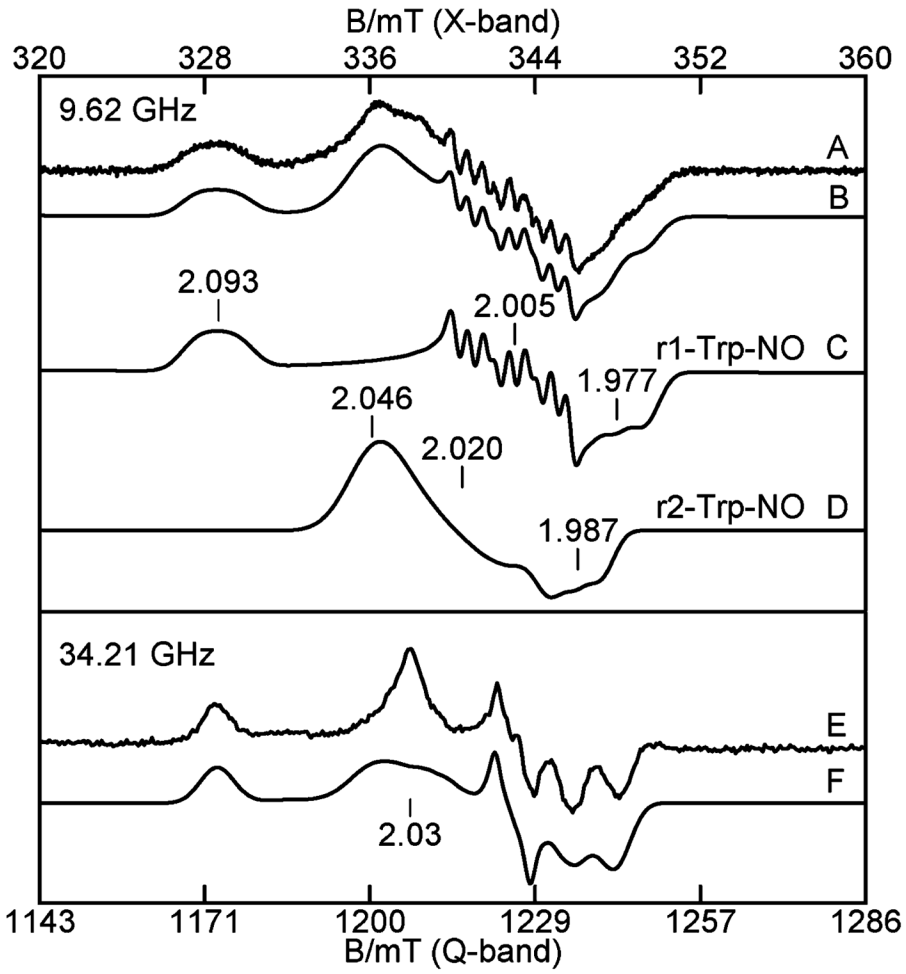

Figure 8.

(A) X- and (E) Q-band EPR spectra of the NO adduct of 0.3 mM reduced TDO with 10 equiv of L-Trp. (B) Simulation sum (C) + (D) for the two sites, (C) simulation of r1-Trp-NO, (D) simulation of r2-Trp-NO, and (F) simulation sum for the two sites of (E). Experimental conditions: microwave frequencies as listed; power, 0.02 mW (X), 0.05 mW (Q); temperature, 20 K (X), 27 K (Q).

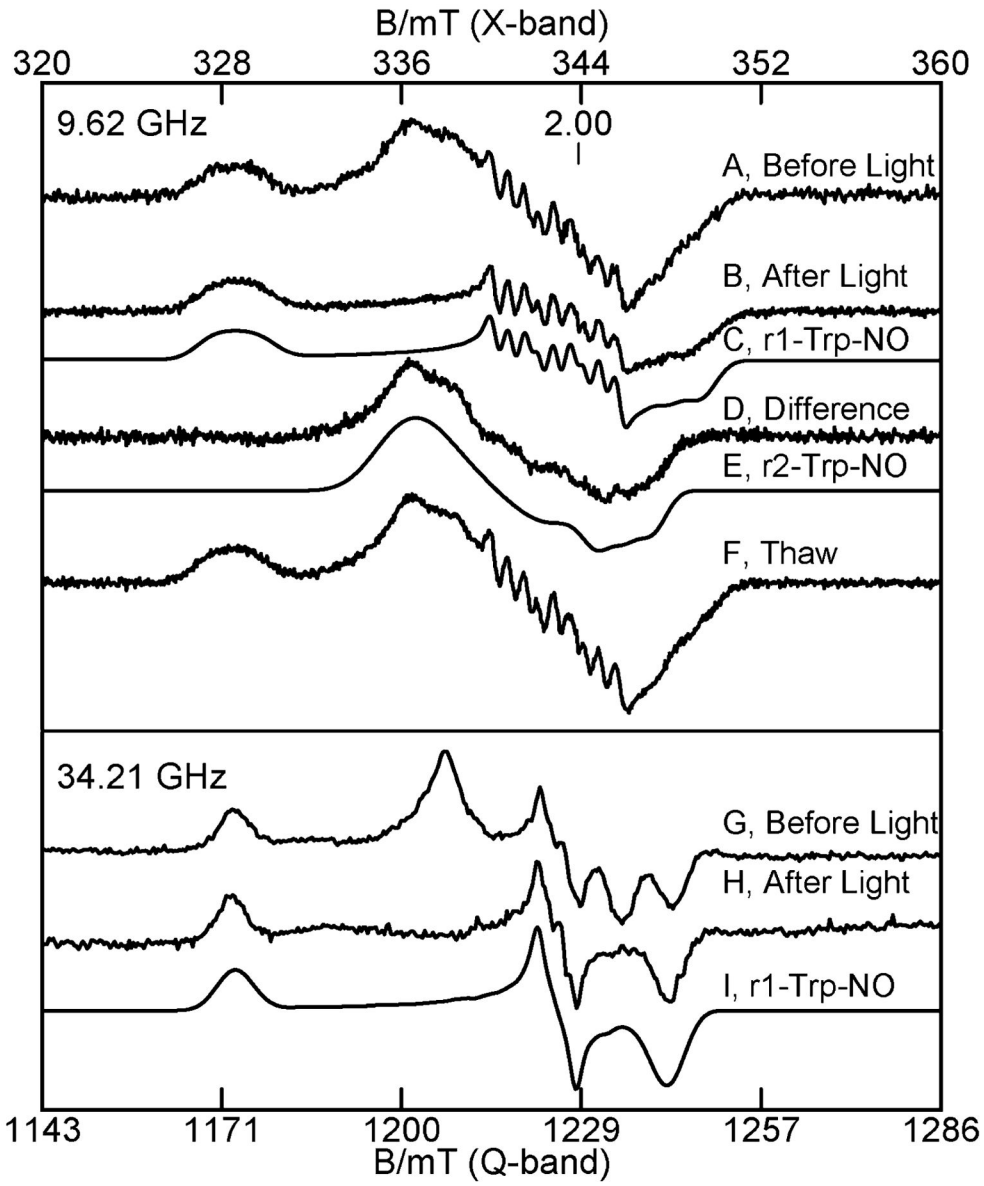

Figure 9.

Photodissociation of the NO adduct from r2-Trp-NO. X- (top part) and Q-band (lower part) EPR spectra of the NO adduct of 0.3 mM reduced TDO with 10 equiv of L-Trp. (A) Before light, (B) after exposure to light at 77 K, (C) simulation of r1-Trp-NO, (D) difference (A)–(B), (E) simulation of r2-Trp-NO, (F) after anaerobic thawing in dark, (G) before light, (H) after exposure to light at 77 K, and (I) simulation of r1-Trp-NO. The experimental conditions and simulation parameters of the species are the same as in Figure 8.

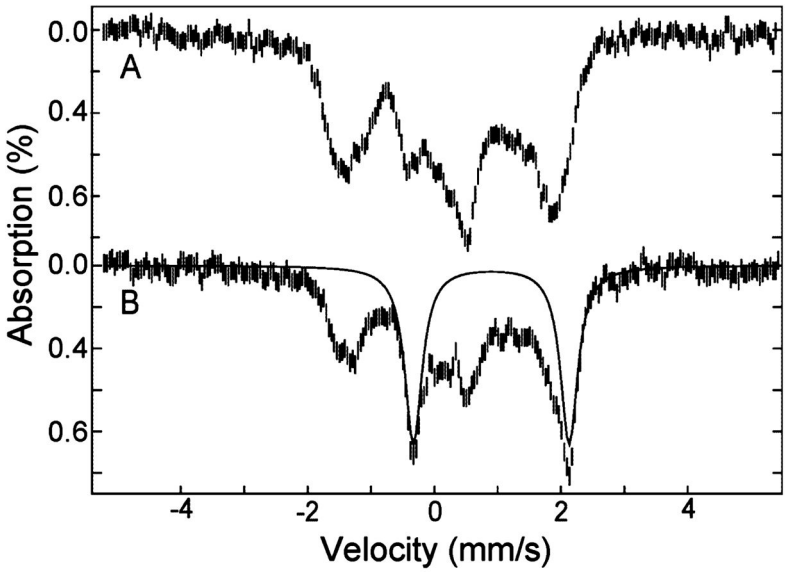

Figure 10.

Mössbauer spectra of (A) 2 mM reduced TDO, pH 7.4, with 10 equiv of L-Trp and excess NO, and (B) after exposure to light for 1 h at 77 K. All spectra were recorded at 4.2 K in a magnetic field of 45 mT parallel to γ-ray direction. The solid line is a simulation with parameters given in the text.

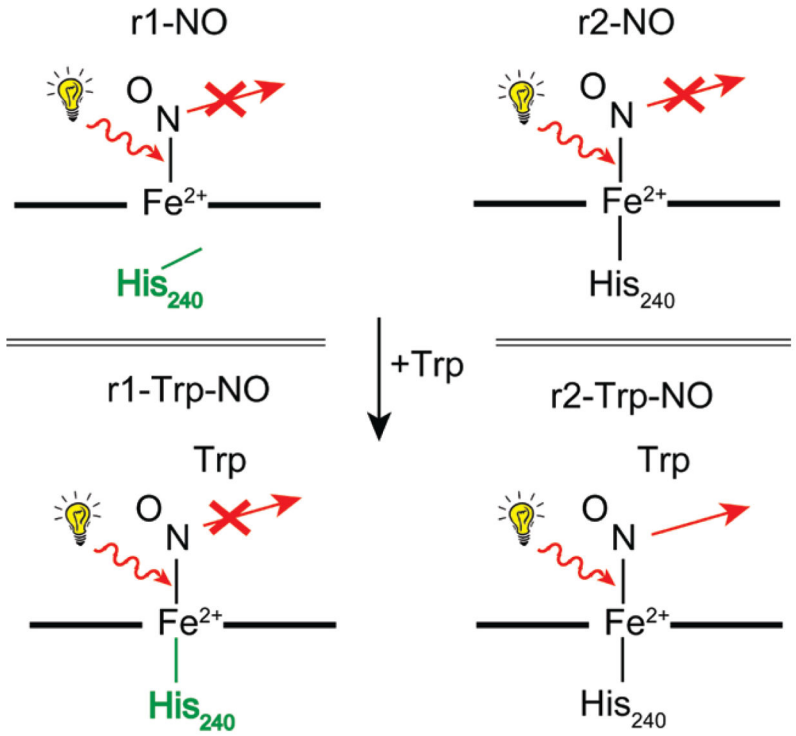

Figure 11.

Spectroscopic states of reduced TDO with NO, highlighting 5- to 6-coordinate conversion of r1-NO with L-Trp, and specific conversion of r2-Trp-NO to r2-Trp after illumination.

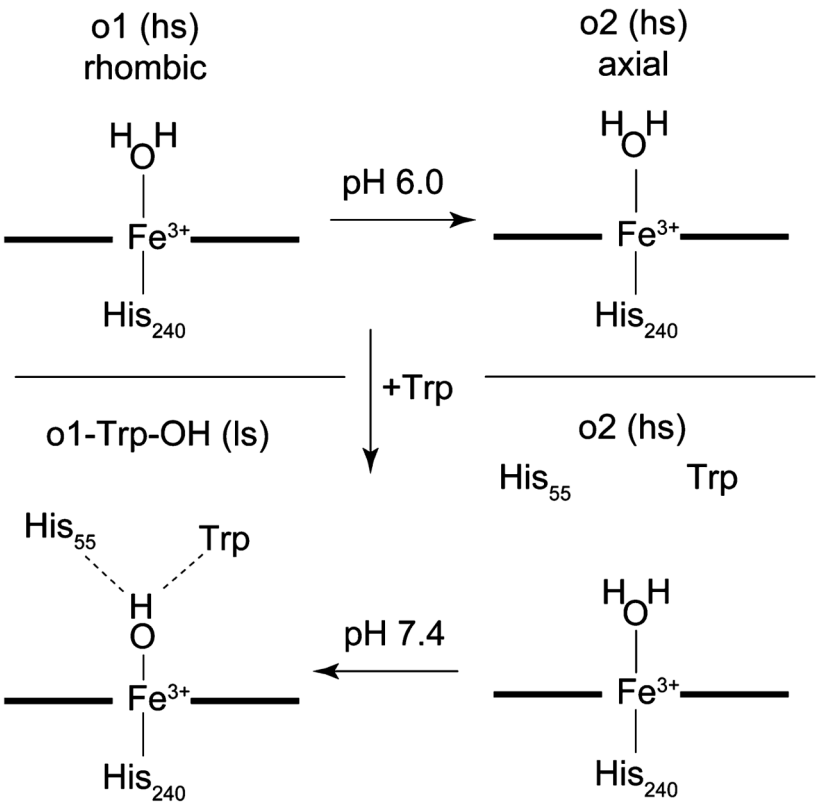

Figure 12.
Spectroscopic states observed for oxidized TDO.

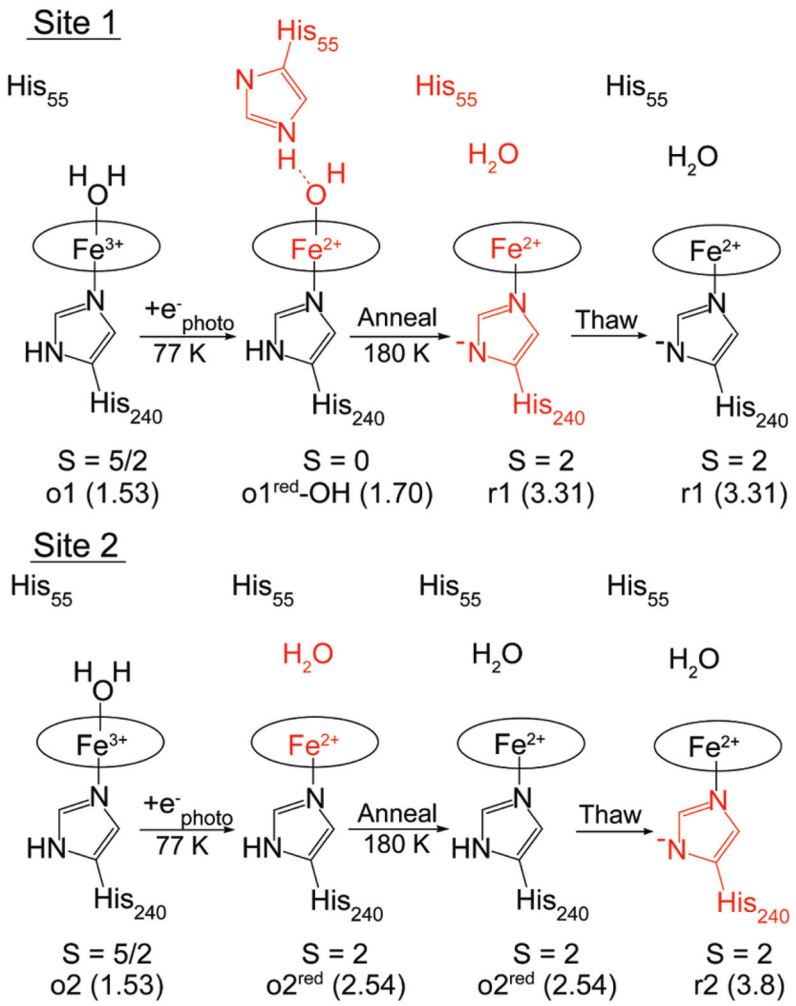

Figure 13.

Heme states observed from the cryoreduction of oxidized TDO with spin states as shown. The numbers in parentheses are the values of ΔE_Q (in mm/s) for the respective states. Red indicates a change from the previous state.

Table 1

EPR Parameters of Oxidized (o) and Reduced (r) Heme Sites 1 and 2 of TDO[a]

state	spin	*g*-tensor	% amount	
o1, o2	5/2	6.18, 5.73, 2.00	100	
o1-Trp-OH	1/2	2.69, 2.19, 1.80	49(5)	$\|\Delta/\lambda\| = 5.02$, $\|V/\Delta\| = 0.86$
o2-Trp	1/2	6.03, 5.78, 2	35(5)	$E/D = 0.006$
o-Trp[b]	5/2	6.63, –, –	7(2)	
o-Trp-OH[b]	1/2	2.61, 2.16, 1.84	9(3)	
r1-NO	1/2	2.110, 2.031, 2.011	50(5)	$A^{NO} = (43, 47, 49)$[c]
r2-NO	1/2	2.105, 2.016, 1.985	50(5)	
r1-Trp-NO	1/2	2.093, 2.005, 1.977	50(5)	$A^{NO} = (33, 56, 41)$, $A^{His} = (–, 21, –)$
r2-Trp-NO	1/2	2.046, 2.020, 1.987	50(5)	

[a] Each row grouping are the heme states in the same protein sample.

[b] Minor species.

[c] *A*-values in MHz.

Table 2

Mössbauer Parameters of Oxidized (o) and Reduced (r) Heme Sites 1 and 2 of TDO[a]

state	spin	δ (mm/s)	ΔE_Q (mm/s)	% amount
o1, o2	5/2	0.42	1.53, $\eta = 0$	100
r1, r2	2	1.0	3.3, 3.8	80(5)
r-minor	2	1.0	2.6	20(5)
r1-Trp	2	1.0	3.1, 3.6	35(5)
r2-Trp	2	0.95	2.54	65(5)[b]
r_a-CO	0	0.29	0.37	50(10)
r_b-CO	0	0.29	0.76	50(10)
$o1^{red}$-OH[c]	0	0.55	1.70, $\eta = 0$	25(3)[d]
$o2^{red}$	2	0.95	2.54	25(5)
$o1^{red}$-anneal	2	1.00	3.31	20(3)[d,e]
$o2^{red}$-anneal	2	0.95	2.54	25(5)

[a] Each row grouping specifies the heme states in the same protein sample.

[b] May contain 20% minor species.

[c] Superscript “red” refers to the cryoreduction of the oxidized state.

[d] 50% of the iron remained ferric.

[e] 5% of the iron remained $o1^{red}$-OH.

Table 3

EPR Parameters of Heme NO Adducts

complex	*g*-tensor	^{14}N *A*-tensor (MHz)	ref
Five-Coordinate Heme–NO Complexes			
TDO(r1-NO)	2.110, 2.031, 2.011	43, 47, 49	tw[a]
cyt *b6f*	2.108, 2.012, 2.003	45, 57, 49	46
cyt c′	2.116, 2.017, 2.008	36, 44, –	47
sGC	2.083, 2.036, 2.012	67, 43, 45	48
FeOEP	2.110, 2.040, 2.012	43, 53, 44	49
FeTPP	2.102, 2.064, 2.010	37, 50, 49	50
Hb_α	2.07, 2.04, 2.008	35, –, 46	31
Six-Coordinate Heme–NO Complexes			
TDO(r2-NO)	2.105, 2.016, 1.985		tw
TDO(r1-Trp-NO)	2.093, 2.005, 1.977	33, 56, 41	tw
TDO(r2-Trp-NO)	2.046, 2.020, 1.987		tw
cyt *c* oxidase a_3	2.092, 2.006, 1.980	29, 62, 31	51
Mb	2.076, 2.007, 1.987	28, 56, 47	51
Imid-FeTPP	2.079, 2.004, 1.972	32, 61, 33	30, 51
Cyt P450	2.068, 2.008, 1.978	–, 56, –	52

[a]This work.